Biochemical and Biophysical Research Communications 733 (2024) 150695

Contents lists available at ScienceDirect

Biochemical and Biophysical Research Communications

journal homepage: www.elsevier.com/locate/ybbrc

Structural insight into sugar-binding modes of microbial ß-amylase

Akira Hirata [a,*], Bunzo Mikami [b,c,**]

[a] Department of Natural Science, Graduate School of Technology, Industrial and Social Science, Tokushima University, 2-1 Minamijosanjimacho, Tokushima, Tokushima, 770-8506, Japan
[b] Laboratory of Metabolic Science of Forest Plants and Microorganisms, Research Institute for Sustainable Humanosphere, Kyoto University, Gokasyo, Uji, Kyoto, 611-0011, Japan
[c] Structural Energy Bioscience, Institute of Advanced Energy, Kyoto University, Gokasyo, Uji, Kyoto, 611-0011, Japan

ARTICLE INFO

Keywords:
β-amylase
Bacillus cereus
Raw-starch digestion
Novel sugar-binding sites
Distorted sugar formation

ABSTRACT

ß-Amylase, which catalyses the release of ß-anomeric maltose from the non-reducing end of starch, is widely used in the food industry. Increasing its enzyme activity through protein engineering might improve the efficiency of food processing. To obtain detailed structural information to assist rationale design, here the crystal structure of *Bacillus cereus* β-amylase (BCB) complexed with maltose was determined by molecular replacement and refined using anisotropic temperature factors to 1.26 Å resolution with R_{work}/R_{free} factors of 12.4/15.7 %. The structure contains six maltose and one glucose molecules, of which two maltose and one glucose are bound at sites not previously observed in BCB structures. These three new sugar-binding sites are located on the surface and likely to be important in enhancing the degradation of raw-starch granules. In the active site of BCB, two maltose molecules are bound in tandem at subsites −2 ~ −1 and +1 ~ +2. Notably, the conformation of the glucose moiety bound at subsite −1 is a mixture of α-anomeric distorted $^{1,4}B$ boat and $^{4}C_1$ chair forms, while those at subsites −2, +1 ~ +2 are all in the $^{4}C_1$ chair forms. The O1 of the distorted α-glucose residue at subsite −1 occupies the position of the putative catalytic water, forming a hydrogen bond with OE1 of Glu367 (base catalyst), suggesting that this distorted sugar is not involved in catalysis. Together, these findings pave the way for further improving the functionality of microbial ß-amylase enzymes.

1. Introduction

Starch is saccharified by various amylolytic enzymes, and the resulting sugars are widely used in the food industry as a nutritional source of energy. ß-Amylase (α-1,4-glucan maltohydrolase; EC 3.2.1.2) catalyses the liberation of ß-anomeric maltose from the non-reducing ends of starch. Maltose has a milder sweetness than sucrose and is used primarily in the production of maltose syrup and in the brewing industry. The enzyme can also be added to processed foods such as bread and rice cakes to prevent starch ageing and to maintain softness [1].

ß-Amylase is a member of family 14 of glycoside hydrolases [2–5] and is distributed in higher plants [6] and some microorganisms [7–9]. In plants, it has physiological roles in seed activation prior to germination, fruit development and ripening [10,11]. Currently, industrial β-amylase is sourced mainly from plants such as soybean and wheat. However, the continued supply of plant β-amylase is an increasing concern due to the rise in grain prices resulting from global economic instability. In this respect, microbial β-amylases are a potential alternative to plant enzymes because they can be easily obtained and have a lower risk of allergy.

There have been extensive structure–function analyses of β-amylases from the genus *Bacillus* [12–14]. The catalytic domain consists of a $(\beta/\alpha)_8$-barrel fold and is very similar to that of plant enzymes. However, the enzyme has a unique starch-binding domain (SBD) [15], not found in plant enzymes, which is assumed to be responsible for degrading raw starch granules. Regarding industrial maltose production, the use of microbial β-amylase might significantly reduce costs by eliminating the need for starch gelatinization at high temperatures [16]. Product development for industrial use of *Bacillus flexus* β-amylase is underway [17], and *Bacillus aryabhattai* β-amylase has also been found to retain high activity and thermal stability [18]. If these β-amylases are made highly functional, their value for industrial use would be further

* Corresponding author.
** Corresponding author. Laboratory of Metabolic Science of Forest Plants and Microorganisms, Research Institute for Sustainable Humanosphere, Kyoto University, Gokasyo, Uji, Kyoto 611-0011, Japan.
E-mail addresses: ahirata@tokushima-u.ac.jp (A. Hirata), b.mikami.kyoto@gmail.com (B. Mikami).

https://doi.org/10.1016/j.bbrc.2024.150695
Received 26 August 2024; Accepted 12 September 2024
Available online 13 September 2024

Table 1
Data collection and refinement statistics of BCB/maltose. Values in parentheses are for the outer shell.

	BCB/Maltose
A. Diffraction data	
X-ray source	SPring-8/BL38B1
Wavelength (Å)	1.0
Resolution range (Å)	50.00–1. 26 (1.28–1. 26)
Space group	$P2_1$
Unit cell parameters	
a, b, c (Å), β (°)	56.974, 89.843, 66.035, 103.092
Unique reflections	171593 (7029)
Multiplicity	3.3 (1.7)
Completeness (%)	99.3 (80.5)
Mean *I*/(*I*)	48.5 (5.95)
Wilson *B*-factor (Å^2)	12.72
R_{merge} (%)	4.7 (18.2)
R_{meas} (%)	5.4 (24.6)
$CC_{1/2}$ (%)	99.5 (94.6)
B. Refinement statistics	
Resolution range used refinement (Å)	10–1.26 (1.30–1.26)
Number of reflections	162442 (13191)
Completeness (%)	93.24 (84.55)
R_{work} (%)	12.4 (21.0)
R_{free} (%)	15.7
Amino acid residues	516 (1–516)
Ca^{2+}/Mal/Glc/SO_4^{2-}/Gol/water	1/6/1/1/8/869
R.m.s.d., bond lengths (Å)	0.02
R.m.s.d., bond angles (Å)	0.04
Ramachandran outliers	3 (Asn243, Tyr398, Thr510)
cis peptide	4 (186–187, 340–341,396–397, 503–504)
PDB ID	8ZRZ

enhanced. An effective way to achieve this is rational design based on the precise structure of the enzyme complexed with substrate analogues.

Herein, we determined the structure of *Bacillus cereus* ß-amylase (BCB)/maltose complex at 1.26 Å resolution, representing a marked improvement to our previously determined resolution of 2.0 Å. Three surface-located sugar-binding sites have been newly identified, as well as an alternative conformation of the sugar bound to the active site. Our findings will pave the way for improving the functionality of microbial ß-amylase enzymes.

2. Materials and methods

2.1. Crystallization and data collection

Overexpression, purification, and crystallization of BCB were performed as described previously [9,12]. In brief, crystallization of BCB was performed at 18 °C by the hanging drop vapor diffusion method as follows: 5 μL of protein solution (15 mg/mL) in 0.05 M sodium acetate buffer was mixed with 5 μL of mother liquor consisting of 15 % PEG6000 and 5 % saturated $(NH_4)_2SO_4$ in 0.1 M phosphate buffer (pH 6.5) containing 300 mM maltose. Drops were allowed to equilibrate to 1 mL of mother liquor for 3 days and then microseeded with BCB crystals. Crystals appeared within 6 h of seeding and grew for 1 week. The BCB crystal used for data collection was approximately 1 mm × 0.5 mm × 0.5 mm and monoclinic. A data set at 1.26 Å resolution was collected at the BL38B1 beamline of SPring-8 using an ADSC Quantum 4R CCD detector and monochromatic wavelength (λ = 1.000 Å) from the flash-frozen crystal at 100 K. Data reduction was performed with HKL2000 [19]. Data collection statistics are summarized in Table 1.

2.2. Structure refinement

Using the coordinates of the previous BCB structure (PDB ID 1B9Z) as a search model, we obtained the molecular replacement phase of the high-resolution crystal structure using AutoSol in Phenix [20]. The model was manually rebuilt using COOT [21] and then further refined with SHELXL [22]. Throughout the whole process, 171,593 reflections (representing 99.3 % of the total data between 10 and 1.26 Å resolution) were used for refinement, and 8582 reflections were reserved for cross-validation analysis using R_{free}. Finally, the structure of BCB was refined to R_{work}/R_{free} residuals of 12.4/15.7 % between 10 and 1.26 Å resolution (Table 1). The main chain torsion angles of three residues (Asn243, Tyr398 and Thr510) were in the outlier region of Ramachandran plots with distinct electron density. Anisotropic refinement of atomic temperature factors except for hydrogen atoms resulted in a significant improvement in the quality of the electron density map, allowing in most cases unambiguous determination of the correct orientation of the side chain residues by distinguishing among carbon, nitrogen and oxygen atoms. The puckering parameters of the sugar rings were calculated by the method of Cremer and People [24] implemented to an internet server [25].

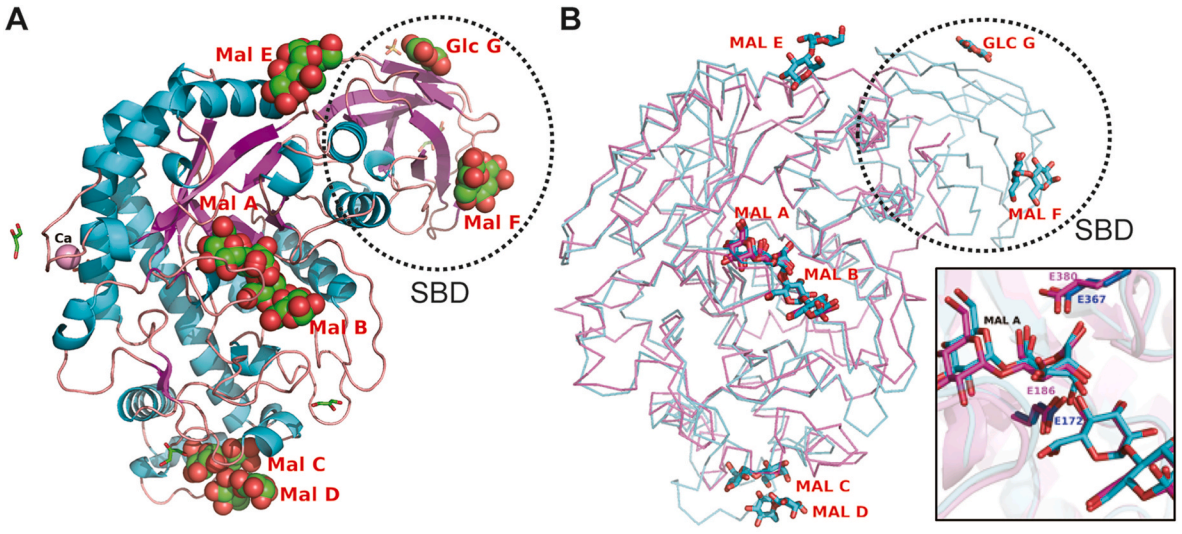

Fig. 1. Whole structure of the BCB/maltose complex. **A**, Cartoon representation with sphere models of maltose (A–F) and glucose (G). **B**, Comparison of BCB (blue) with soybean β-amylase (magenta). Inset shows the magnified active site. The starch-binding domain (SBD) is shown as a dotted circle. (For interpretation of the references to colour in this figure legend, the reader is referred to the Web version of this article.)

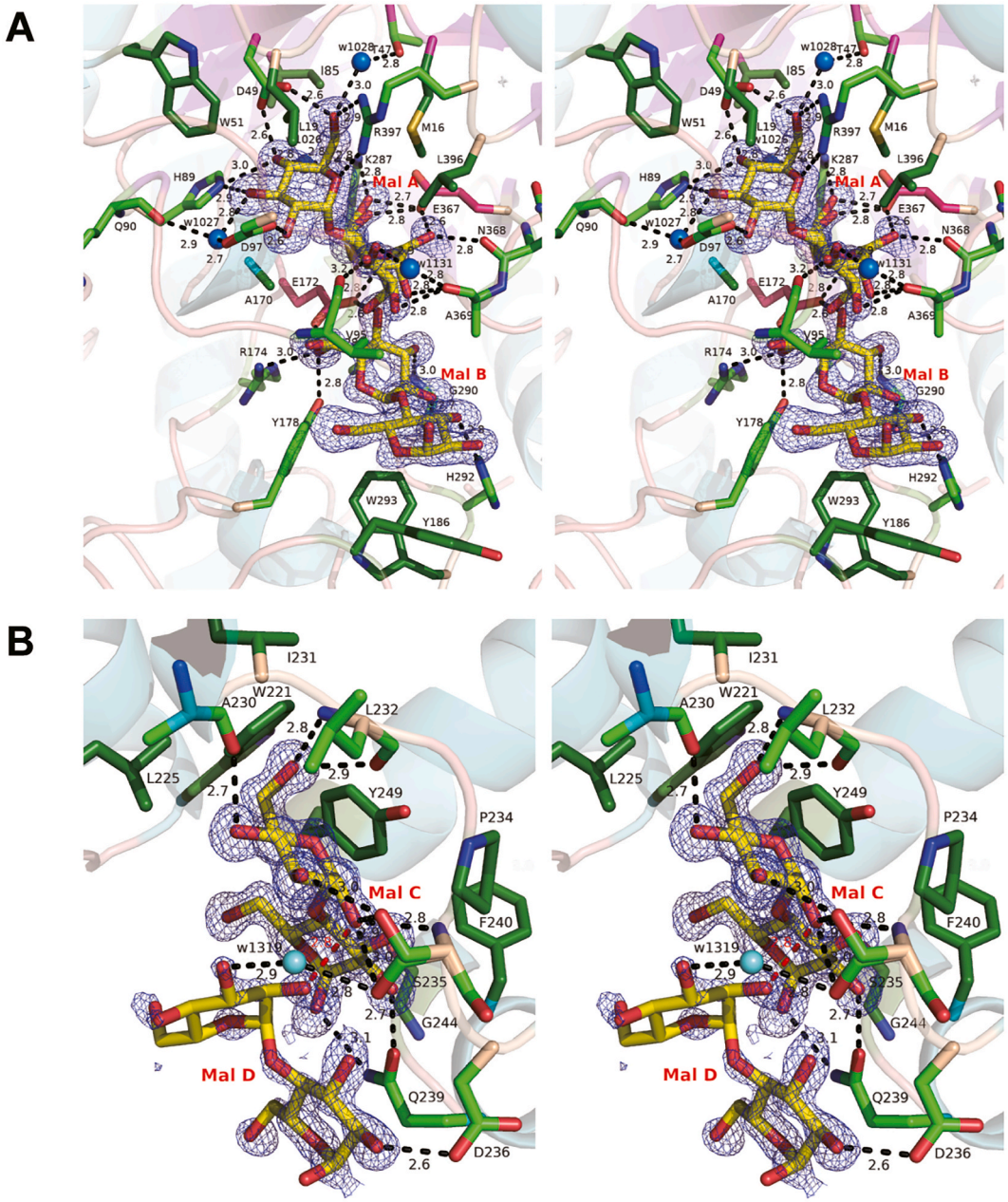

Fig. 2. Maltose-binding sites with Fo–Fc omit map contoured at 3 δ. **A**, Mal A and Mal B in the active site; **B**, Mal C and Mal D. Left and right stereo images are shown.

2.3. Sequence analysis

Sequence analysis was performed using sequences from *Bacillus cereus* (WP_018780455.1), *Bacillus flexus* (RIV10038.1), *Bacillus aryabhattai* (WP_033580731.1), and *Bacillus megaterium* (AJI22868). The alignment was prepared using Clustal W [26] and ESPript3 [27].

3. Results and discussion

3.1. Overall structure and sugar-binding sites

The BCB/maltose complex crystallized in space group $P2_1$ with dimensions of $a = 56.97$, $b = 89.84$, and $c = 66.04$ Å. The structure was solved by molecular replacement and refined to 1.26 Å resolution (Table 1). The final model contains 516 residues, six maltose, one glucose, one calcium ion, one sulfate ion, nine glycerols and 890 water molecules. The flexible loop (92–96), which is reported to play an important role in the catalytic step [23], is in the closed form. In contrast, the inner loop (329–332) is a mixture of apo and product forms [23].

The structure consists of two domains: the N-terminal catalytic domain and the C-terminal SBD (Fig. 1A). The catalytic domain adopts a $(\beta/\alpha)_8$-barrel fold, as previously reported [12], whereas the SBD consists of two 4-stranded antiparallel β-sheets, which are classified as carbohydrate-binding module 20 (CBM20) [28]. Only microbial β-amylases possess the SBD, while the structure of the N-terminal catalytic domain is conserved between BCB and soybean amylase (SBA) (Fig. 1B).

Two maltose molecules, Mal A (Glc4-3, chain B) and Mal B(Glc2-1, chain B) are bound consecutively at subsites $-2 \sim -1$ and $+1 \sim +2$ in the active site. In addition to these, there are three maltose residues bound in the catalytic domain. Two maltose molecules Mal C (Glc2-1, chain C) and Mal D (Glc2-1, chain D) are bound to one sugar-binding site in the hook-like domain in the loop region (L4) between β4 and α4 of the $(\beta/\alpha)_8$ barrel. Although the binding mode of Mal C is almost the same as

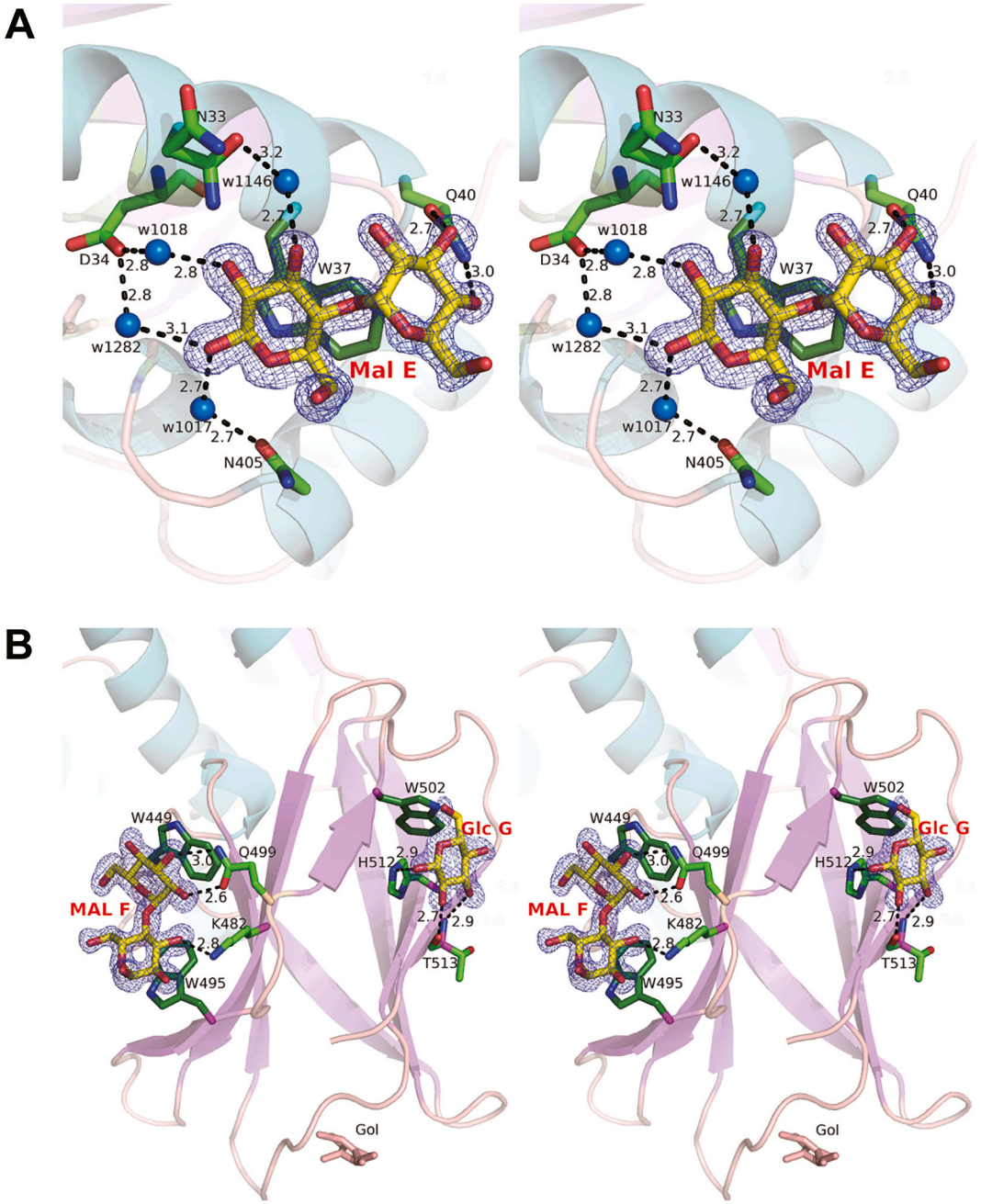

Fig. 3. Maltose-binding sites with Fo–Fc omit map contoured at 3 δ. **A**, Mal E; **B**, SBD Mal F and Glc G in the SBD domain. Left and right stereo images are shown.

that observed previously in BCB, Mal D is newly observed on the outer side of Mal C with the diffused density of the non-reducing end glucose residue. Another novel maltose, Mal E (Glc2-1, chain E) is located between α1 and α8 of the $(\beta/\alpha)_8$ barrel. In contrast to the catalytic domain, only one maltose, Mal F (Glc2-1, chain F) and one glucose, Glc G (Bgc602, cain A) are found at the surface of SBD. Mal F is located around strands βb3 and βb4, while Glc G is located about 19 Å away from Mal F between strands βb4 and βa4.

The isotropic temperature factors, occupancies, puckering parameters, sugar ring forms, anomer types and sugar torsion angles of the six maltose molecules and glucose residue are summarized in Supplementary Table 1. Except for a glucose residue with an alternate $^{1,4}B$ conformation at subsite −1, the sugar conformations of the other glucose residues are in the $^{4}C_1$ chair form. Of the maltose-binding sites, Mal D shows the lowest occupancy. The glucose residues in the active site have the lowest isotropic B-factor (14.0 Å^2 for site −2 and 15.2 Å^2 for site +2), while the reducing end of Mal F has the highest isotropic B-factor (33.8 Å^2). The reducing ends of Mal A–Mal D and Mal F are all α-anomeric, while those of Mal E and Glc G are β-anomeric (Bgc residues). The sugar torsion angles of the six maltose molecules are all in the stable regions [29].

3.2. *Maltose in the active site with a distorted glucose ring*

In our BCB/maltose complex structure (Fig. 2A), the sugar-ring of the glucose at subsite −1 has two alternate ring forms: the $^{1,4}B$ boat configuration (occ. 0.75) and the $^{4}C_1$ chair configuration (occ. 0.25). Both forms are the α-anomer (Supplementary Table 1). Based on the atomic distance, the interactions between the glucose residues and protein residues comprise hydrogen bonds and C–C contacts

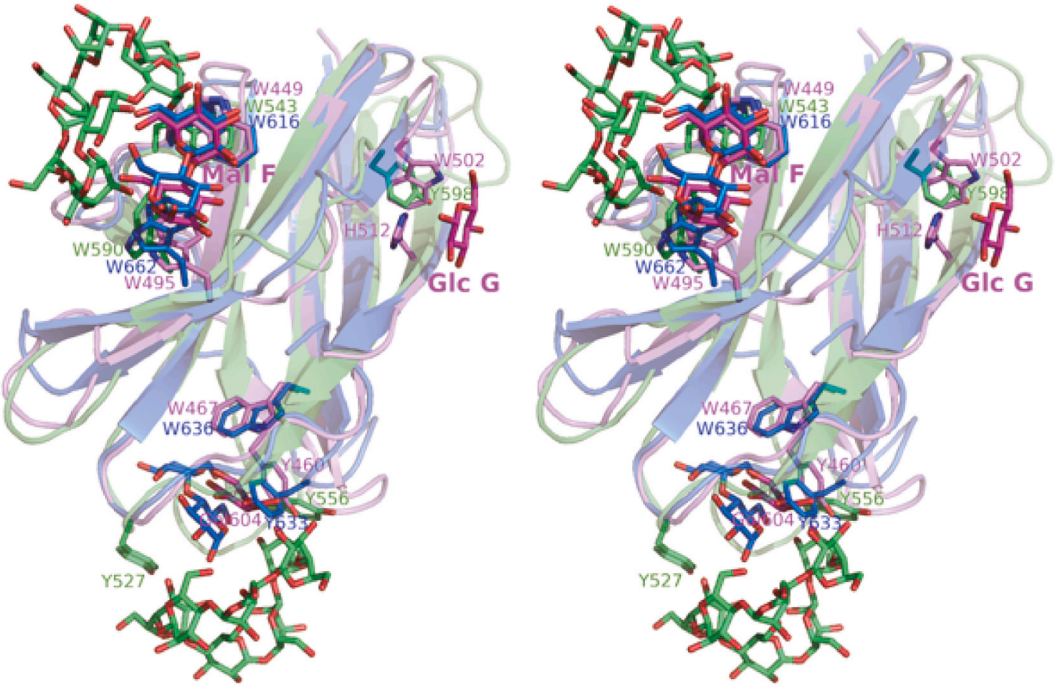

Fig. 4. Comparison of the carbohydrate-binding motif CBM20 in BCB (pink), CGTase (blue, PDB ID 1CDG) and glucoamylase (green, PDB ID 1AC0). BCB and CGTase are complexed with maltose; glucoamylase is complexed with β-cyclodextrin. The r.m.s.d values are 1.18 Å (100 Cα), 2.82 Å (100 Cα) and 2.51 Å (102 Cα) between BCB and CGTase, between BCB and glucoamylase, and between CGTase and glucoamylase, respectively. The Mal F site of BCB is common to CGTase and glucoamylase. The disordered Gol 604 site of BCB also seems to be common to CGTase and glucoamylase, but the Glc G site of BCB is specific to β-amylase. Left and right stereo images are shown. (For interpretation of the references to colour in this figure legend, the reader is referred to the Web version of this article.)

(Supplementary Table 2). The interactions of the glucose residues at the active site (subsite −2 ~ +2) are almost the same as those reported previously [12], except for the glucose at subsite −1, which is α-anomeric and shows the novel ^{1,4}B boat and $^{4}C_1$ chair configurations. In the previous low-resolution refinement, the glucose at subsite −1 was the β-anomer with a $^{4}C_1$ chair configuration. Here, O1′ of the glucose with the ^{1,4}B boat configuration is placed close to the position of the catalytic water molecule, allowing it to create a hydrogen bond with OE2 of Glu367 (base catalyst) and O of Asn368, while the O1' of the glucose with the $^{4}C_1$ chair configuration makes a hydrogen bond with the acid catalyst of Glu172 (Supplementary Table 2). This suggests that the base catalyst is important not only to activate the catalytic water, but also to distort the sugar-ring at the −1 site of Mal B. In a previous study of SBA, it was concluded that formation of the ^{1,4}B boat configuration at −1 site depends on pH higher than the pK_a of the base catalyst [30]. The α-anomeric ^{1,4}B boat configuration seems to be related to the inhibition of β-amylase by its product maltose, because the K_i value of maltose is reported to be around 6 mM in SBA [31]. This suggests that the distorted sugar may be useful for the design of a specific inhibitor of β-amylase. The difference in architecture around the base catalyst between BCB and SBA is thought to be due to variations in the optimum pH of the respective enzymes [30,32].

3.3. Maltose-binding sites in the catalytic domain

As mentioned above, two maltose molecules (Mal C and Mal D) are bound to the sugar-binding site in the hook-like domain in the loop region (L4) between β4 and α4 of the $(\beta/\alpha)_8$ barrel (Fig. 1). The interactions between the maltose molecules and the protein residues are depicted in Fig. 2B and summarized in Supplementary Table 2. The newly observed Mal D is close to Mal C. Mal D makes one hydrogen bond with OD2 of Asp236, and a water-mediated hydrogen bond with OG of Ser235. The glucose residue at the reducing end of Mal D make C–C contacts with Asp236 and Gln239. Mal D is positioned almost parallel to Mal C in the same direction, making one hydrogen bond between O2 of Mal C and O2 of Mal D. This binding mode of Mal C and Mal D seems to be important for recognition of the branched chains of starch, although the occupancy of the Mal D site is low (0.45). The other novel maltose (Mal E) is located between α1 and α8 of the $(\beta/\alpha)_8$ barrel (Fig. 3A). The glucose residue at the non-reducing end of Mal E make hydrogen bonds with Gln40 (O3···Gln40 OD2 and O4···Gln40 NE2), while that at the reducing end of Mal E makes water-mediated hydrogen bonds with Asn33 O and Asn405 OD1 (Supplementary Table 2). The side chain of Trp37 forms C–C contacts with the two glucose residues of Mal E.

3.4. Maltose-binding sites in SBD

In addition to the sugars in the catalytic domain, one maltose (Mal F) and one glucose residue (Glc G) are present at the surface of SBD (Fig. 3B). Mal F is located around strands of βb3 and βb4 as reported previously [15]; however, Glc G is newly identified between strands βb4 and βa4 at a distance of ~19Å from Mal F. Glc G forms CH/π-stacking interaction with His 512 and C–C contacts with Trp502. It also makes two hydrogen bonds with the main-chain O and N of Thr513 (Fig. 3B and Supplementary Table 1). The position of Glc G is distinct from maltose-binding site 2 found in the SBD of cycrodextrin glycosyltransferase (CGTase) [33,34] and glucoamylase (GA) [35] (Fig. 4). Similar to the SBD of CGTase and GA, these two sugar-binding sites in SBD of BCB may be important in promoting the degradation of raw starch.

3.5. Significance of the sugar-binding sites of BCB

The novel sugar-binding sites (Mal D, Mal E and Glc G), located at non-catalytic surface regions of the catalytic domain and SBD, were not observed in previous structures of BCB/maltose. Co-crystallization with higher maltose concentration, as used in the present study, seems to find weak binding sites better than the previous soaking method [12].

Similar binding sites, termed surface binding sites (SBSs), have been observed in various types of α-amylases and are usually formed by an aromatic residue on the surface of the enzyme [36,37]. Extensive mutational analyses of several types of α-amylases suggest that stacking interactions between the sugar ring and the aromatic residue at the SBSs are essential to the adsorption of starch and also increase catalytic activity, especially towards insoluble starch. Therefore, it is possible that the SBSs in BCB weakly absorb starch granules to promote interaction of the enzyme with its substrate and enhance degradation of starch by the SBD. Indeed, such weak binding sites seem to be correlated with the digestion of raw starch by amylolytic enzymes. In general, the interaction between the carbohydrate binding motif and carbohydrate is weak, thereby making the interaction easily reversible. Notably, the amino acid residues comprising the three novel binding sites are mostly conserved in the genus *Bacillus* (Supplementary Fig. 1), but not in other genera. This indicates that the ability of β-amylase of the genus *Bacillus* to degrade starch granules is superior to that of others, and that improving the three binding sites may further increase enzyme activity.

4. Conclusions

Our high-resolution structure of BCB/maltose complex has revealed three sugar-binding sites (Mal D, Mal E and Glc G) not seen in the previous structure. It is likely that these binding sites function as SBSs, as observed in various α-amylases, and may contribute to the degradation of starch granules by adsorbing starch. Further increasing the ability of the SBSs to adsorb starch, by using protein engineering to introduce aromatic amino acids for stacking interactions with sugars or to arrange amino acid residues to form hydrogen bonds, might lead to higher raw starch degrading activity. Our structure also reveals that the glucose in subsite −1 in the active site of BCB takes disordered conformations. One is the α-anomer $^{4}C_{1}$ chair form and the other is the α-anomer $^{1,4}B$ boat conformation. O1 of the boat form makes a hydrogen bond between the O1 of glucose and the base catalyst (Glu367). This α-anomer configuration indicates that excess maltose production may lead to the inhibition of β-amylase, resolving a long-standing issue.

Data availability

The crystal structure of the BCB/maltose is deposited on Protein Data Banka (PDB) with accession code 8ZRZ.

CRediT authorship contribution statement

Akira Hirata: Conceptualization, Funding acquisition, Investigation, Supervision, Validation, Writing – original draft, Writing – review & editing. **Bunzo Mikami:** Conceptualization, Data curation, Formal analysis, Funding acquisition, Investigation, Project administration, Visualization, Writing – review & editing.

Declaration of competing interest

The authors declare that they have no known competing financial interests or personal relationships that could have appeared to influence the work reported in this paper.

Acknowledgments

The authors thank the staff members of the beamline facility at SPring-8 (Hyogo, Japan) for their technical support during data collection. The synchrotron radiation experiment was performed at BL38B1 in the SPring-8 with the approval of 2002B0799. This work is partially supported by JSPS KAKENHI [grant numbers 22K05441 and 24K09352].

Appendix A. Supplementary data

Supplementary data to this article can be found online at https://doi.org/10.1016/j.bbrc.2024.150695.

References

[1] H. Taniguchi, Y. Honnda, Amylases, in: Encyclopedia of Microbiology, Elsevier, 2009, pp. 159–173, https://doi.org/10.1016/B978-012373944-5.00130-9.
[2] B. Henrissat, A classification of glycosyl hydrolases based on amino acid sequence similarities, Biochem. J. 280 (1991) 309–316, https://doi.org/10.1042/bj2800309.
[3] B. Henrissat, I. Callebaut, S. Fabrega, P. Lehn, J.P. Mornon, G. Davies, Conserved catalytic machinery and the prediction of a common fold for several families of glycosyl hydrolases, Proc. Natl. Acad. Sci. USA 92 (1995) 7090–7094, https://doi.org/10.1073/pnas.92.15.7090.
[4] B. Henrissat, G. Davies, Structural and sequence-based classification of glycoside hydrolases, Curr. Opin. Struct. Biol. 7 (1997) 637–644, https://doi.org/10.1016/s0959-440x(97)80072-3.
[5] V. Lombard, H. Golaconda Ramulu, E. Drula, P.M. Coutinho, B. Henrissat, The carbohydrate-active enzymes database (CAZy) in 2013, Nucleic Acids Res. 42 (2014) D490–D495, https://doi.org/10.1093/nar/gkt1178.
[6] J.A. Thoma, J.E. Spradlin, S. Dygert, in: The Enzyme, third ed., Academic Press, New York, 1971.
[7] M. Higashihara, S. Okada, Studies on *β*-amylase of *Bacillus megaterium* strain No. 32, Agric. Biol. Chem. 38 (1974) 1023–1029, https://doi.org/10.1080/00021369.1974.10861268.
[8] M. Hoshino, Y. Hirpse, K. Sano, K. Mitsugi, Adsorption of microbial *β*-amylase on starch, Agric. Biol. Chem. 39 (1975) 2415–2416, https://doi.org/10.1271/bbb1961.39.2415.
[9] T. Nanmori, M. Nagai, Y. Shimizu, R. Shinke, B. Mikami, Cloning of the beta-amylase gene from *Bacillus cereus* and characteristics of the primary structure of the enzyme, Appl. Environ. Microbiol. 59 (1993) 623–627, https://doi.org/10.1128/aem.59.2.623-627.1993.
[10] H. Zhang, W.-B. Shen, W. Zhang, L.-L. Xu, A rapid response of *β*-amylase to nitric oxide but not gibberellin in wheat seeds during the early stage of germination, Planta 220 (2005) 708–716, https://doi.org/10.1007/s00425-004-1390-7.
[11] L. Wang, M. Jing, S. Gu, D. Li, X. Dai, Z. Chen, J. Chen, Genome-wide investigation of BAM gene family in annona atemoya: evolution and expression network profiles during fruit ripening, Int. J. Mol. Sci. 24 (2023) 10516, https://doi.org/10.3390/ijms241310516.
[12] B. Mikami, M. Adachi, T. Kage, E. Sarikaya, T. Nanmori, R. Shinke, S. Utsumi, Structure of raw starch-digesting *Bacillus cereus* beta-amylase complexed with maltose, Biochemistry 38 (1999) 7050–7061, https://doi.org/10.1021/bi9829377.
[13] T. Oyama, M. Kusunoki, Y. Kishimoto, Y. Takasaki, Y. Nitta, Crystal structure of beta-amylase from Bacillus cereus var. mycoides at 2.2 A resolution, J. Biochem. 125 (1999) 1120–1130, https://doi.org/10.1093/oxfordjournals.jbchem.a022394.
[14] H. Miyake, G. Kurisu, M. Kusunoki, S. Nishimura, S. Kitamura, Y. Nitta, Crystal structure of a catalytic site mutant of beta-amylase from *Bacillus cereus* var. mycoides cocrystallized with maltopentaose, Biochemistry 42 (2003) 5574–5581, https://doi.org/10.1021/bi020712x.
[15] H.-J. Yoon, A. Hirata, M. Adachi, A. Sekine, S. Utsumi, B. Mikami, Structure of the starch-binding domain of *Bacillus cereus* β-amylase, J. Microbiol. Biotechnol. 9 (1999) 619–623. http://jmb.or.kr/journal/view.html?uid=635&vmd=Full.
[16] H. Sun, P. Zhao, X. Ge, Y. Xia, Z. Hao, J. Liu, M. Peng, Recent advances in microbial raw starch degrading enzymes, Appl. Biochem. Biotechnol. 160 (2010) 988–1003, https://doi.org/10.1007/s12010-009-8579-y.
[17] E. and P.A. (CEP) EFSA Panel on Food Contact Materials, V. Silano, J.M. Barat Baviera, C. Bolognesi, P.S. Cocconcelli, R. Crebelli, D.M. Gott, K. Grob, C. Lambré, E. Lampi, M. Mengelers, A. Mortensen, G. Rivière, I.-L. Steffensen, C. Tlustos, H. Van Loveren, L. Vernis, H. Zorn, L. Herman, J. Aguilera, M. Andryszkiewicz, D. Arcella, N. Kovalkovicova, Y. Liu, A. Chesson, Safety evaluation of the food enzyme β-amylase from *Bacillus flexus* strain AE-BAF, EFSA J. 19 (2021) e06635, https://doi.org/10.2903/j.efsa.2021.6635.
[18] X. Duan, Q. Zhu, X. Zhang, Z. Shen, Y. Huang, Expression, biochemical and structural characterization of high-specific-activity β-amylase from Bacillus aryabhattai GEL-09 for application in starch hydrolysis, Microb. Cell Factories 20 (2021) 182, https://doi.org/10.1186/s12934-021-01649-5.
[19] Z. Otwinowski, W. Minor, Processing of X-ray diffraction data collected in oscillation mode, Methods Enzymol. 276 (1997) 307–326, https://doi.org/10.1016/S0076-6879(97)76066-X.
[20] T.C. Terwilliger, Improving macromolecular atomic models at moderate resolution by automated iterative model building, statistical density modification and refinement, Acta Crystallogr D Biol Crystallogr 59 (2003) 1174–1182, https://doi.org/10.1107/s0907444903009922.
[21] P. Emsley, K. Cowtan, Coot: model-building tools for molecular graphics, Acta Crystallogr D Biol Crystallogr 60 (2004) 2126–2132, https://doi.org/10.1107/S0907444904019158.
[22] G.M. Sheldrick, T.R. Schneider, SHELXL: high-resolution refinement, Methods Enzymol. 277 (1997) 319–343, https://doi.org/10.1016/S0076-6879(97)77018-6.
[23] Y.-N. Kang, A. Tanabe, M. Adachi, S. Utsumi, B. Mikami, Structural analysis of threonine 342 mutants of soybean β-amylase: role of a conformational change of the inner loop in the catalytic mechanism, Biochemistry 44 (2005) 5106–5116, https://doi.org/10.1021/bi0476580.

[24] D. Cremer, J.A. Pople, A general definition of ring puckering coordinates, J. Am. Chem. Soc. 97 (1975) 1354–1358, https://doi.org/10.1021/ja00839a011.
[25] S. Fushinobu, Cremer-Pople Parameter Calculator [Internet], 2006. Available from: https://enzyme13.bt.a.u-tokyo.ac.jp/CP.
[26] R. Chenna, H. Sugawara, T. Koike, R. Lopez, T.J. Gibson, D.G. Higgins, J. D. Thompson, Multiple sequence alignment with the Clustal series of programs, Nucleic Acids Res. 31 (2003) 3497–3500, https://doi.org/10.1093/nar/gkg500.
[27] P. Gouet, X. Robert, E. Courcelle, ESPript/ENDscript: extracting and rendering sequence and 3D information from atomic structures of proteins, Nucleic Acids Res. 31 (2003) 3320–3323, https://doi.org/10.1093/nar/gkg556.
[28] A.B. Boraston, D.N. Bolam, H.J. Gilbert, G.J. Davies, Carbohydrate-binding modules: fine-tuning polysaccharide recognition, Biochem. J. 382 (2004) 769–781, https://doi.org/10.1042/BJ20040892.
[29] A. Imberty, S. Perez, A revisit to the three-dimensional structure of B-type starch, Biopolymers 27 (1988) 1205–1221, https://doi.org/10.1002/bip.360270803.
[30] A. Hirata, M. Adachi, A. Sekine, Y.-N. Kang, S. Utsumi, B. Mikami, Structural and enzymatic analysis of soybean β-amylase mutants with increased pH optimum, J. Biol. Chem. 279 (2004) 7287–7295, https://doi.org/10.1074/jbc.M309411200.
[31] K. Nomura, B. Mikami, Y. Morita, Interaction of soybean β-amy1ase with glucose, J. Biochem. 100 (1986) 1175–1183, https://doi.org/10.1093/oxfordjournals.jbchem.a121821.
[32] A. Hirata, M. Adachi, S. Utsumi, B. Mikami, Engineering of the pH optimum of *Bacillus cereus* β-amylase: conversion of the pH optimum from a bacterial type to a higher-plant type, Biochemistry 43 (2004) 12523–12531, https://doi.org/10.1021/bi049173h.
[33] C.L. Lawson, R. van Montfort, B. Strokopytov, H.J. Rozeboom, K.H. Kalk, G.E. de Vries, D. Penninga, L. Dijkhuizen, B.W. Dijkstra, Nucleotide sequence and X-ray structure of cyclodextrin glycosyltransferase from *Bacillus circulans* strain 251 in a maltose-dependent crystal form, J. Mol. Biol. 236 (1994) 590–600, https://doi.org/10.1006/jmbi.1994.1168.
[34] R.M. Knegtel, B. Strokopytov, D. Penninga, O.G. Faber, H.J. Rozeboom, K.H. Kalk, L. Dijkhuizen, B.W. Dijkstra, Crystallographic studies of the interaction of cyclodextrin glycosyltransferase from Bacillus circulans strain 251 with natural substrates and products, J. Biol. Chem. 270 (1995) 29256–29264, https://doi.org/10.1074/jbc.270.49.29256.
[35] K. Sorimachi, M.F. Le Gal-Coëffet, G. Williamson, D.B. Archer, M.P. Williamson, Solution structure of the granular starch binding domain of Aspergillus Niger glucoamylase bound to beta-cyclodextrin, Structure 5 (1997) 647–661, https://doi.org/10.1016/s0969-2126(97)00220-7.
[36] D. Cockburn, C. Wilkens, C. Ruzanski, S. Andersen, J. Willum Nielsen, A.M. Smith, R.A. Field, M. Willemoës, M. Abou Hachem, B. Svensson, Analysis of surface binding sites (SBSs) in carbohydrate active enzymes with focus on glycoside hydrolase families 13 and 77 — a mini-review, Biologia (Bratisl) 69 (2014) 705–712, https://doi.org/10.2478/s11756-014-0373-9.
[37] U. Baroroh, M. Yusuf, S.D. Rachman, S. Ishmayana, M.R.A.A. Syamsunarno, J. Levita, T. Subroto, The importance of surface-binding site towards starch-adsorptivity level in α -amylase: a review on structural point of view, Enzym. Res. 2017 (2017) 1–11, https://doi.org/10.1155/2017/4086845.